# Finite Element Analysis for Understanding Oil and Gas Well Deformation Mechanisms

Jueren Xie, Cam Matthews, Thomas Dessein

C-FER Technologies, Canada

***Abstract****: Based on documented field experience worldwide, oil and gas wells in a wide range of applications are subject to significant casing deformation damage due to a variety of causal loading and/or geological setting conditions. In many cases, the casing deformations have occurred as a result of mechanical or formation movement loading conditions associated with the well completion/stimulation activities and/or the recovery process. Severe casing deformations can lead to the loss of casing structural or seal integrity or restricted well access resulting in a well failure condition.*

*Finite Element Analysis (FEA) is often used to achieve a better understanding of the relevant well deformation mechanisms and risks for applications where severe casing deformations have been experienced or may be anticipated. Based on various inputs related to the operational and formation movement loading conditions, advanced non-linear FEA can be used to predict the nature and magnitude of the casing deformation response over the service life of a well. Such modeling, in conjunction with caliper survey diagnostic information, can serve to confirm the validity of specific well deformation postulations, and to assist in devising effective mitigation strategies based on well design, construction and/or process modifications.*

*This paper presents several FEA models used to analyze different modes of casing deformation including casing collapse, buckling and shear. Analysis examples are presented to demonstrate the use of the FEA models together with available caliper survey data in investigating the loading conditions and mechanisms responsible for causing such casing deformations in a number of actual wells.*

***Keywords****: Analysis, Buckling, Caliper-log, Casing, Collapse, Curvature, Deformation, Design, Failure, Flexural Strain, Formation, Oilwell, Plasticity, Sand, Shale, Shear, Stiffness, Strain, Stress, Yield Strength*

## 1. Introduction

Field experience has demonstrated that oil and gas wells can be exposed to significant casing deformation damage risk in a wide range of applications including:

- enhanced and thermal recovery operations;
- geothermal wells;
- hydraulically fractured or stimulated wells;
- subsidence prone reservoirs including diatomites, weak chalks and unconsolidated sands where massive sand production occurs (e.g. cold heavy oil wells); and

- subsalt reservoirs.

The damage risk also extends to field developments in regions that are tectonically active or overlain by a thick permafrost layer.

The casing deformations occur due to a number of different loading mechanisms which, in many cases, are associated with the well completion/stimulation activities and/or recovery process. These include high pressure differential conditions, significant thermal strain cycles and loading introduced by formation movements of varying types and magnitude. For example, Figure 1 shows a schematic of a horizontal well which is prone to formation shear loading at both uphole and reservoir top positions corresponding to relatively weak bedding plane interfaces which can experience various amounts of slip in conjunction with reservoir expansion or fracturing under a thermal recovery process. Such well configurations, which include vertical, build and horizontal sections, are commonly used today for producing unconventional shale and heavy oil reservoirs. Severe casing deformations may lead to the impairment or loss of casing string structural or leakage integrity (e.g. parting, collapse, connection damage) or well serviceability (e.g. restricted or complete loss of well access).

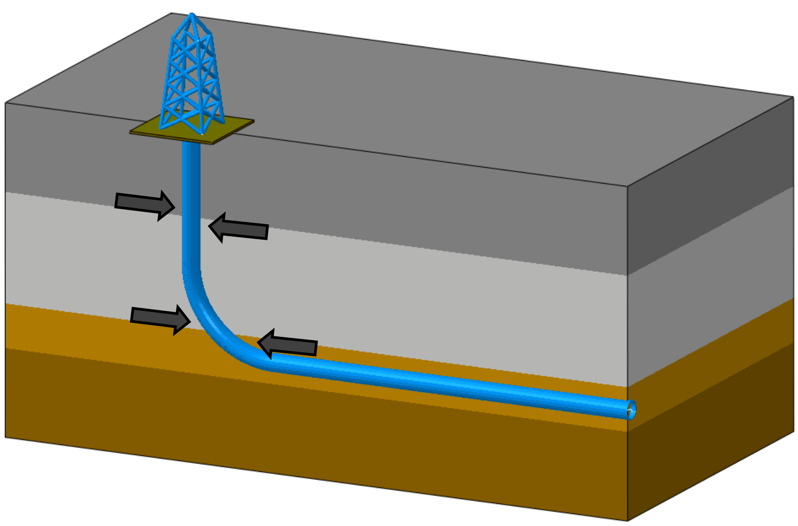

**Figure 1 Schematic of a Horizontal Well Susceptible to Formation Shear Movement**

An understanding of the relevant well deformation mechanisms and risks is essential to devise effective mitigation strategies based on well design, construction and/or process modifications. When a well is suspected to have sustained severe casing damage at one or more locations, operators will typically run various diagnostic surveys to obtain data which characterizes the nature and extent of the damage. This often includes the use of multi-arm caliper logs which provide direct measurements of the well deformation features as described in further detail below. The caliper survey data can be used in conjunction with other relevant information to postulate whether a particular well deformation feature reflects a collapse, buckling or shear loading situation, and to what extent various causal mechanisms may have played a role. However, such interpretations are generally of a qualitative nature and sometimes they can be misleading. Therefore, further confirmation of the deformation conditions and causal factors through quantitative engineering and/or analytical evaluations is often warranted.

Finite Element Analysis (FEA) is often used to achieve a better understanding of observed well casing deformations and to perform casing design/optimization assessments for applications where deformations may be anticipated (i.e. classic design methodologies do not address such loading conditions). Based on various inputs related to the operational and formation movement loading conditions, advanced non-linear FEA can be used to predict the nature and magnitude of the casing deformation response over the service life of a well. Therefore, the use of FEA, in conjunction with certain caliper survey diagnostic data, can serve to confirm the validity of specific well deformation postulations, and to assist in the identification and development of effective strategies for well deformation mitigation.

This paper presents several FEA models used to analyze different modes of casing deformation including casing collapse, buckling and shear. Analysis examples are presented to demonstrate the use of the FEA models in conjunction with processed caliper survey data in investigating the loading conditions and mechanisms responsible for causing such casing deformations in a number of actual wells.

## 2. Caliper-log Survey of Well Deformations

Multi-finger caliper logs are often run to identify and assess well casing deformations, although a more typical objective for the multi-finger caliper tools is to obtain wall loss measurements due to corrosion and wear in wellbore tubulars. Once a caliper tool is lowered to the bottom of a well segment to be logged, spring-loaded caliper fingers are extended to make contact with the internal surface of the pipe body and the tool is then pulled up at a prescribed speed and the movements of the individual fingers are logged. The caliper tools are typically deployed in a well as part of an assembly which includes centralizers at each end comprised of stiff springs that serve to keep the tool aligned with the pipe axis. This tool configuration generally leads to eccentricity between the tool center and the tubular axis when the tool passes through a well deformation such as a buckle or shear, as shown in Figure 2. This measured eccentricity and ovality of the cross-sectional profile at each depth can be interpreted using an iterative deconvolution algorithm to determine the actual local well trajectory.

Depending on the tool design, the multi-finger caliper surveys provide up to 60 independent measurements of the casing inner radius logged with a depth resolution of less than 1 mm. The caliper data can be processed using mathematical and statistical algorithms (i.e. software) to accurately determine the local trajectory of the logged tubular string. The processed results include strain, ovality, trajectory and three-dimensional visualization information for the logged tubular to gain a more quantitative understanding of the type and magnitude of any deformation features that exist along the well. This allows for a consistent interpretation methodology that may be applied across a wide variety of wells which have experienced deformations.

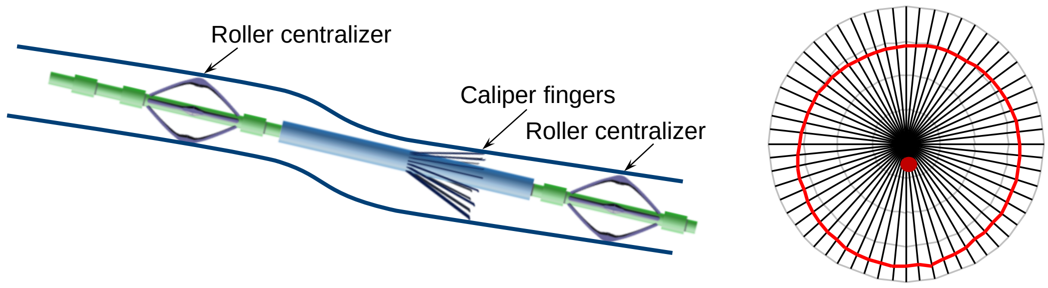


**Figure 2  Caliper Tool Eccentricity Within a Deformed Wellbore**
**(a) Caliper Finger Offset; (b) Cross-Section Showing Pipe Centre Offset**

Quantified characterization of the deformed shape of the casing or tubing strings at discrete locations along a wellbore provides critical information about the form and magnitude of the deformation feature.  This information can be used to examine the potential for individual deformation features to cause access limitations or to impact wellbore structural integrity through potential loss of hydraulic isolation.  Such characterizations also provide an understanding of the underlying mechanisms responsible for the deformation occurrence in a particular application (see list of relevant application scenarios above).

The algorithms use the caliper tool geometry and the measured ovality and eccentricity relative to the pipe center, as shown in Figure 2, to calculate the local curvature of the pipe at each survey station.  The curvature and well orientation determined at each station are then assembled by the software to describe the local well trajectory.

The results from multi-finger caliper data analyses can be used to postulate the likely cause of a well deformation feature.  Figure 3 shows actual examples of deformation features identified in different wells that were postulated to have been caused by collapse, lateral buckling, helical buckling and formation shear conditions in the respective wells.  In some cases, the characteristics of a deformation feature may also suggest that the damage occurred as a result of some combination of operational load and formation movement conditions.  The wellbore deformation characteristics presented in Figure 3 also demonstrate how the analysis can be used to identify and interpret such features by magnifying changes in radius, trajectory and cross-section.

The processing algorithms employed within the caliper analysis software were validated and enhanced through full scale testing with the test set-up shown in Figure 4(a).  The ability of these algorithms to accurately predict tubular deformations based on multi-finger caliper tool measurements was demonstrated by confirming agreement between the calculated trajectories and external measurements of a range of controlled pipe deformations as indicated by the example shown in Figure 4(b).

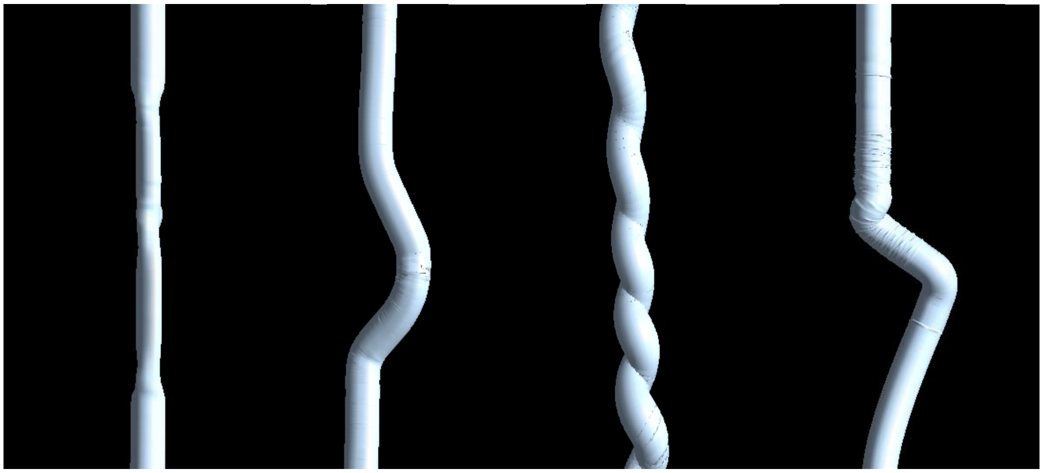

(a) Collapse (b) Lateral Buckling (c) Helical Buckling (d) Shear

**Figure 3 Types of Well Deformation Features (with Magnification)**

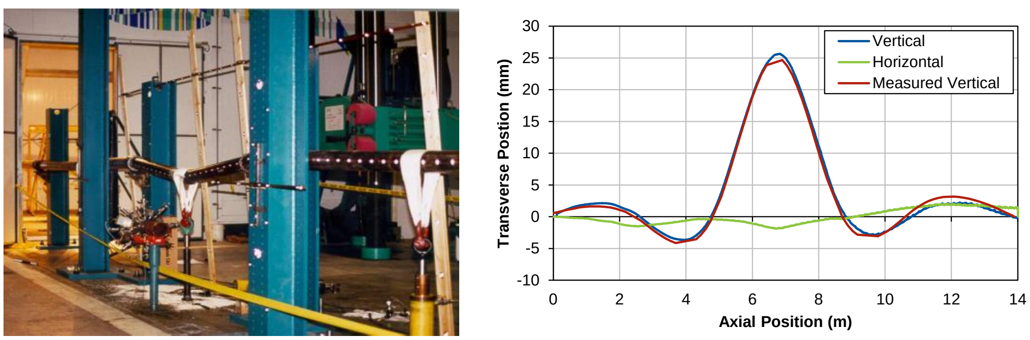


(a) Full Scale Lab Tests (b) Test vs. Software Results

**Figure 4 Calculated vs. Measured Trajectory Validation**

## 3. Casing Design Approaches and Load Conditions

The basic design objective for casing strings in oil and gas wells is to ensure that both structural and leakage integrity will be maintained throughout the well life under the entire range of loading conditions that may be anticipated. Classic casing and tubing string design methods (API 5C3, 2008) employ a Working Stress Design (WSD) or deterministic approach, wherein the loads and nominal strengths are estimated and the design process compares the established loads to the relevant casing or tubing strength values. The outcome must satisfy a minimum specified safety factor for each particular load case. In all cases, the objective of such structural designs is to select a tubular size, weight and grade and connection that will ensure the stress conditions within the string remain below the material yield strength and the connection load capacity. However, such methods have limited utility for the unconventional well types and application conditions that are the subject of this paper given the very severe loading conditions and likely development of inelastic strains. In these applications, it is more prudent to utilize a strain-based tubular design methodology which takes into account structural integrity as well as serviceability requirements (e.g. access or drift limitations, connection leakage limits, etc.).

In designing a casing or tubing string for the unconventional well and application scenarios mentioned above, the following loading conditions should be taken into consideration as appropriate:

- axial tension and compression;
- internal pressure differential (burst);
- external pressure differential (collapse);
- bending (due to well curvature or potential deformations);
- temperature differentials (including thermal cycling);
- pressure cycling (e.g. multi-stage fracturing);
- bending-rotational fatigue (e.g. connections in horizontal wells);
- formation movements (typically strain controlled loading); and
- relevant combined load conditions.

In applying a strain-based design methodology, the casing strain magnitude can be defined as the total longitudinal strain along the casing axis, including both axial strain and flexural strain:

$$\varepsilon = \varepsilon_{Axial} + \varepsilon_{Flexural}$$

Note that axial and flexural strains can be introduced by installation loads, such as hanging weight, buoyancy force and wellbore curvature, operational loads such as temperature and pressure differentials and formation movements. The maximum strains introduced by these respective load conditions will typically vary along the wellbore length and therefore the most critical locations should be identified and evaluated accordingly. The allowable casing strain is often defined by wellbore serviceability requirements and the structural integrity limits of casing connections. Xie (2006) proposed a casing strain design limit of 1.5% for general use in applying a strain-based design methodology.

Due to the plastic loading conditions and non-linear material response, FEA is often used to assist in the design of well tubulars in conjunction with a strain-based design methodology. In such cases, the casing material should be modeled using elastic-plastic relationships with both time and temperature dependencies taken into account. The material model input data will include the elastic modulus, Poisson’s ratio, yield strength, and post-yield stress-strain relationship, each specified as a function of time and temperature.

Several FEA studies have been published previously describing the modeling of tubular string deformations for unconventional well load conditions such as heavy oil and compacting reservoir applications (Xie et al 1999, 2006, 2007 and 2008).

The following sections present several analysis examples of different types of inelastic casing loading and deformations. For the casing deformation cases studied in this paper, the FEA was performed using the commercial software Abaqus R.2016 (2016).

# 4. Analysis of Casing Collapse

## 4.1 FEA Models for Casing Collapse

Two- or three-dimensional FEA can be performed for analyzing casing collapse response under external pressure loading conditions associated with fluid (hydraulic) and/or formation pressure application. While collapse loading due to fluid pressure is almost always treated as being uniform around the pipe circumference, formation-induced collapse loading may be non-uniform (e.g. salt creep, overburden loading applied to horizontal well liners in thermal recovery wells, etc.). For two-dimensional FEA evaluations, a representative cross-section of the casing can be modeled using two-dimensional generalized plane strain elements, allowing the impact of both external pressure and axial loading to be taken into consideration. For three-dimensional FEA evaluations typically used in cases where the loading or boundary conditions vary along the tubular axis, casing collapse is typically modeled using 3D shell elements. A 3D model may also include cement and formation elements, and in order to control the problem size, only a representative length of interest is typically included in the model.

When performing casing collapse analyses, an appropriate initial ovality should be introduced to the model prior to applying the collapse loading conditions. The collapse analysis can be performed using the Riks method (Abaqus 2016) to facilitate accurate prediction of the peak pressure condition and the subsequent reduction in allowable pressure as the ovality increases further in a typical collapse deformation response. In addition, non-uniform external pressure load conditions tend to be more severe than uniform pressures from a collapse resistance perspective, and should be analyzed whenever such loading may be applicable.

## 4.2 Field Example - Casing Collapse

A casing design example for a Western Canada thermal well is considered here. The Steam Assisted Gravity Drainage (SAGD) technology is used for producing bitumen at a depth of approximately 400 m TVD. The production casing string of the SAGD horizontal well must be designed to sustain the cyclic thermal loading resulting from temperature variations between the initial ground temperature of 10°C and the peak steam injection temperature of 290°C. Since the casing string will be constrained axially by the cement and formation, it will be subjected to axial compressive loading during heating and to axial tensile loading during cooling. The post yield material properties and corresponding high temperature effects impact the magnitude of the peak compressive and tensile strains introduced to the casing string during this process.

The design calls for the SAGD well to be completed with a 244.5 mm, 59.5 kg/m L80 production casing that is fully cemented to surface. According to industry design guidelines for thermal wells, the casing collapse resistance should be greater than the maximum relevant formation fracture pressure (DACC 2012).

A two-dimensional FEA model was used to establish the relationship that exists between increasing external pressure and casing ovality, thereby also determining the casing collapse resistance. The casing ovality is defined as the difference between the maximum and minimum casing diameter (i.e. of the deformed configuration at each load step) relative to the original un-deformed diameter. An initial ovality of 0.25% was applied to the FEA model, and the casing section was restrained axially in order to simulate the thermal strains introduced by the thermal cycle loading conditions. To be conservative, no internal pressure was applied. The L80 casing material was modeled using an elastic-plastic constitutive relationship with a Young's modulus of 200 GPa, and yield strengths of 579 MPa at 10˚C and 457 MPa at 290˚C, respectively.

The following three loading scenarios were considered:

- external pressure applied prior to thermal cycle loading;
- external pressure applied after heating when the casing string is subjected to high axial compressive loading; and
- external pressure applied after cooling when the casing string is subjected to high axial tensile loading.

Figure 5 presents the relationship established between external pressure and ovality for these three load scenarios based on FEA performed using the Riks method. A small arc-length with an equivalent load increment of 0.2 MPa was used to improve the accuracy of the analysis results. Due to the limited degrees of freedoms (DOF) inherent to the 2D model, each analysis was completed in a few minutes. Figure 6 presents contour plots of the effective stresses within the casing at different stages of external pressure loading for the case with the external pressure applied prior to the initiation of thermal cycle loading. For clarity, the casing cross-sections presented in Figure 6 show the predicted casing deformations magnified by 10 times.

As shown in Figure 5, the casing ovality initially increases linearly at low external pressure differentials in all three load scenarios. The response starts to become non-linear at an external pressure of about 7.5 MPa, and to become highly non-linear at pressures above 15 MPa. As the casing ovality increases further, a peak external pressure is reached in each case which represents the pipe collapse resistance under the respective load conditions. As indicated in Figure 5, the collapse resistance values are 21.3 MPa, 18.8 MPa and 18.5 MPa for the cases with external pressure applied prior to thermal cycle loading, after heating and after cooling, respectively.

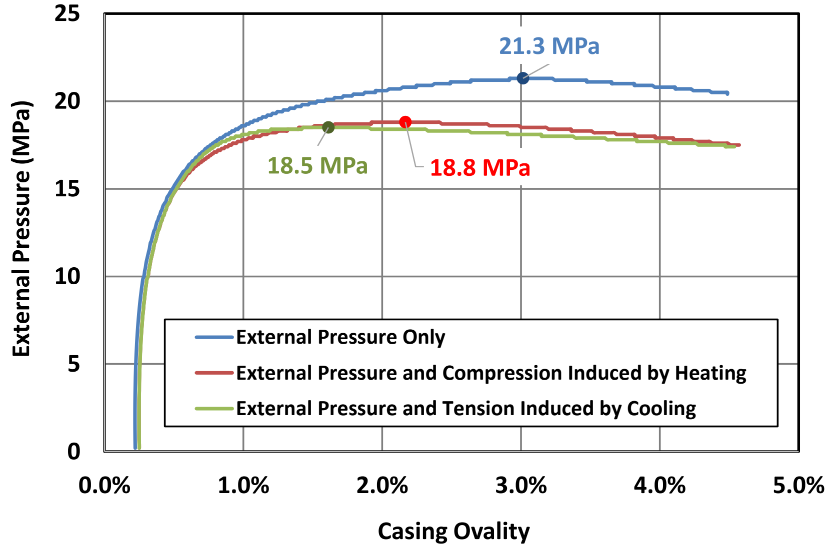


**Figure 5 FEA Results - Casing Ovality vs. External Pressure**

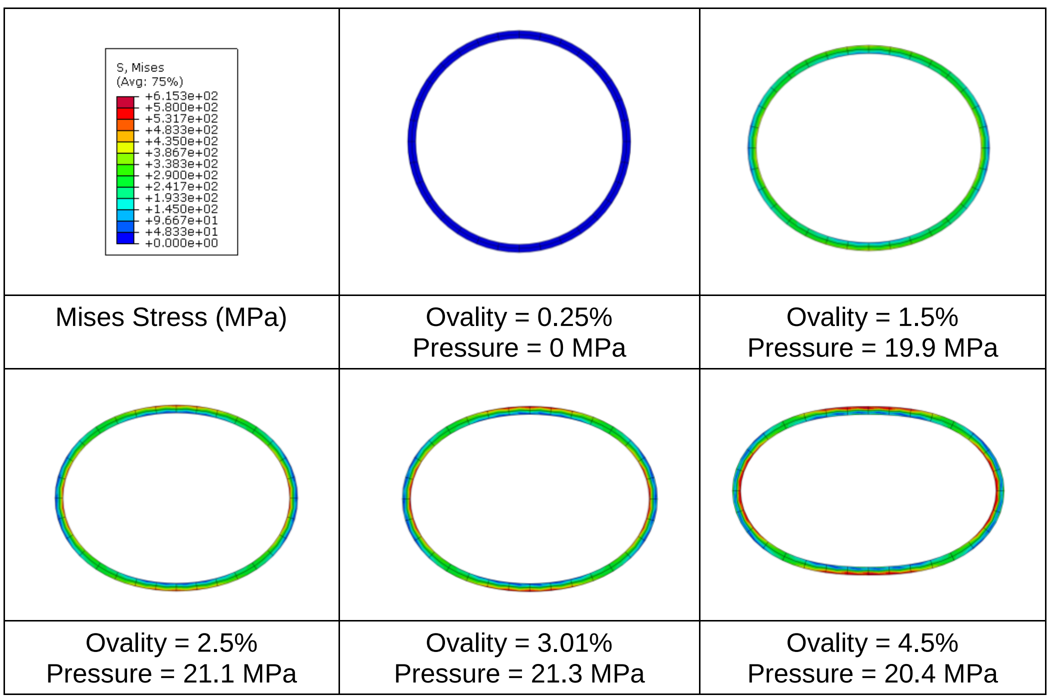


**Figure 6 FEA Results - Effective Stress for Casing under External Pressure Applied Prior to Thermal Cycle Loading**

The reduced collapse resistance after cooling can be attributed to the presence of high axial tensile loading in the constrained casing string. As noted in API 5C3 (2008), the effect of axial tensile loading is required to be taken into account in calculating casing collapse resistance. In contrast, while of a similar magnitude, the decrease in the collapse resistance after heating was caused by the reduction in the yield strength of the L80 material at the high temperature. This example demonstrates the importance of considering the impact of both axial loading and high temperature exposure in calculating the collapse resistance of casing strings.

In Western Canada SAGD developments, the formation fracture pressure in the McMurray formation is approximately 8.8 MPa at a depth of 400 m TVD. Therefore, the predicted collapse resistance of the 244.5 mm, 59.5 kg/m L80 production casing satisfies the design requirements for this SAGD well application.

# 5. Analysis of Casing Buckling

## 5.1 FEA Models for Casing Buckling

Casing and tubing strings are subject to buckling deformations in wells where excessive axial compressive loading occurs, such as in the case of significant formation compaction due to pressure draw-down in weak formations, severe sand production or permafrost thaw subsidence. There are two basic modes of tubular string buckling observed in such wells including single-plane lateral buckling with single or multiple waves, and helical buckling of unsupported segments of inner tubular strings or casing segments within poorly cemented intervals or intervals with very weak formation support.

Figure 7 shows a schematic diagram of the FEA models developed for analyzing the buckling response of casing to load and support conditions that cause either in-plane or helical buckling modes. For in-plane buckling, as shown in Figure 7(a), the casing can be modeled using 2-node beam elements with a pipe cross-section. The model usually covers the entire thickness of the compacting reservoir, and the compaction displacements are applied in steps at the top end of the model. The cement/formation material is modeled using spring elements which apply loads perpendicular to the casing axis. Each spring element consists of a casing-end node and a formation-end node. The casing-end nodes are attached to a casing element and the formation-end nodes are fixed. Since the compaction-induced interval shortening is simulated by applying vertical displacements to the ends of the casing, the model can be used to establish the relationship between the casing flexural strain (bending) and the casing axial strain (axial compression). Note that in some cases, the vertical compaction-induced displacement (loads) may vary through the formation interval, and longitudinal springs will need to be added to the FEA model to facilitate the application of distributed vertical displacements (Xie 2006).

To assess helical buckling, as shown in Figure 7(b), the casing string can be modeled using three-dimensional beam elements which are capable of tracking large out-of-plane deformations. For analyses of unsupported inner tubular string buckling, a discrete annular gap is prescribed between the tubular outside diameter and the surrounding casing string which is assumed to provide a rigid radial support boundary. The interaction between the buckled tubular and the rigid casing surface is modeled using pipe-in-pipe contact elements (Abaqus 2016). For the modeling of casing helical buckling within poorly cemented or very weak formation intervals, the outside radial boundary is characterized as providing a variable weak to strong radial support condition. In the FEA model, the outside boundary for the helical buckling can be specified as either a rigid surface or a deformable solid body.

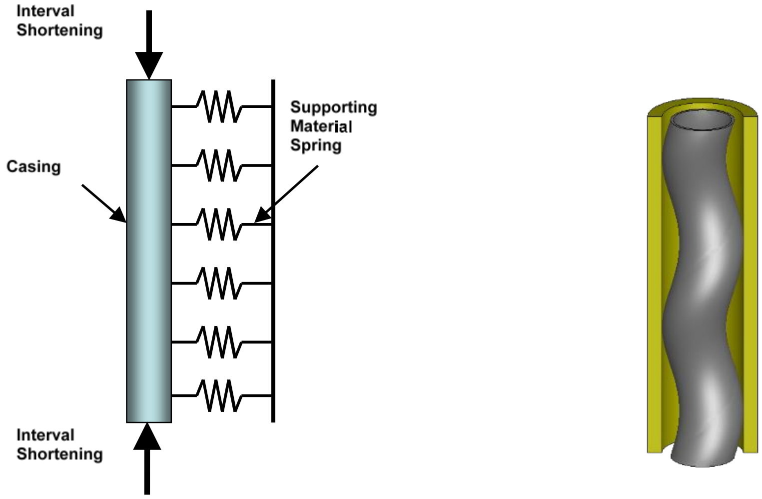


(a) Lateral Buckling (b) Helical Buckling

**Figure 7 Schematic Diagram of FEA Models for Casing Buckling**

## 5.2 Example Case - Casing Buckling

An illustrative example of casing buckling experienced in an HPHT well in an offshore field is considered here. The well was completed with the 177.8 mm, 63.5 kg/m Q125 production casing over a total measured depth of about 6000 m. After six years of operation, a caliper log survey identified a deformation feature with significant curvature over a ~10 m long interval at a depth of approximately 5000 m. The caliper software analysis characterized the deformation feature as having multiple in-plane buckling waves with an average pitch length of 1.35 m. The maximum localized casing curvature was found to be very severe with a magnitude of 195°/30m.

An FEA model was developed to simulate the casing buckling response observed in the well. The Q125 casing material was modeled using an elastic-plastic constitutive relationship with a Young's modulus of 200 GPa, and a yield strength of 862 MPa. The material model included strain-hardening behavior in the post-yield stage with the mechanical properties defined based on available coupon test results. The 10 m long compaction interval corresponding to the wellbore axis was modeled in the analysis (i.e. since the wellbore orientation relative to vertical was not considered, the predicted compaction displacements reflect movements parallel to the well axis). Also, while the analysis did not include the initial loading conditions of the casing (i.e. stresses upon installation at the depth of interest), the impact on the results was considered to be less significant than the formation loads.

The casing buckling FEA served two purposes as follows:

- Determination of the formation spring stiffness:

  For the in-plane buckling mode, the buckle pitch length is dependent on the size, weight and grade of the casing as well as the stiffness of the formation that provides lateral support to the string. Accordingly, the formation spring stiffness could be estimated by matching the results of the numerical buckling simulations to the pitch length of the buckled casing segment established by the caliper survey analysis. Note that the existence of a relationship between buckle pitch length and formation stiffness under elastic loading conditions was also demonstrated by Timoshenko (1972) and Hetenyi (1974).

- Determination of the casing axial strain and formation compaction magnitude:

  The degree of curvature and buckle shape are determined by the amount of shortening that occurs over the formation interval that experiences compressive strains and subsidence (thickness reduction). Therefore, by using the estimated formation stiffness determined in the first step of the analysis, the effects of interval shortening on the casing flexural strain due to buckling can be evaluated. Then, by comparing the casing flexural strain derived from the caliper log analysis to the relationship established between flexural strain and interval shortening, the total compaction magnitude and casing axial strain can be estimated for the subject interval in the well. With the estimated casing total strain, which is the sum of axial strain and flexural strain, an evaluation can be performed to assess the structural integrity and serviceability state of the casing and connections within this interval.

Figure 8 presents the relationship established between casing buckle pitch length and the supporting material stiffness based on the FEA results, corresponding to the condition where the axial stress reaches the casing material yield strength. The pink symbols represent the FEA results, and the blue solid line is the best-fit trend-line. The predicted response shows that the casing buckle pitch length decreases exponentially with increased formation stiffness. The FEA results show some scatter in the pitch length vs. formation spring stiffness relationship, primarily due to the fact that the pitch length is calculated using the model length divided by the discrete integer number of waves.

Since the caliper survey analysis showed multiple in-plane buckling waves with an average pitch length of 1.35 m, the formation spring stiffness was estimated to be 145 N/mm2 based on the relationship shown in Figure 8. This formation spring stiffness is relatively low and can be considered representative of a soft formation. Note that this estimation is based on the assumption that the casing axial stress is at the yield strength, which is reasonable for the case studied here. However, for situations where it is suspected that the casing axial stress is not close to the yield strength and the pitch lengths established by the FEA results do not match the observed values, iterative analyses may be required to determine a more suitable value for the formation stiffness.

Figure 9 presents the relationship established between the curvature of the buckled casing and the total compaction of the formation layer based on the FEA results. Figure 10 shows casing curvature contour plots corresponding to a number of axial strain conditions. For better visualization, the casing deformations in the contour plots have been magnified by 10 times. The casing lateral displacement at 140 mm of formation compaction is 3.5 mm based on FEA.

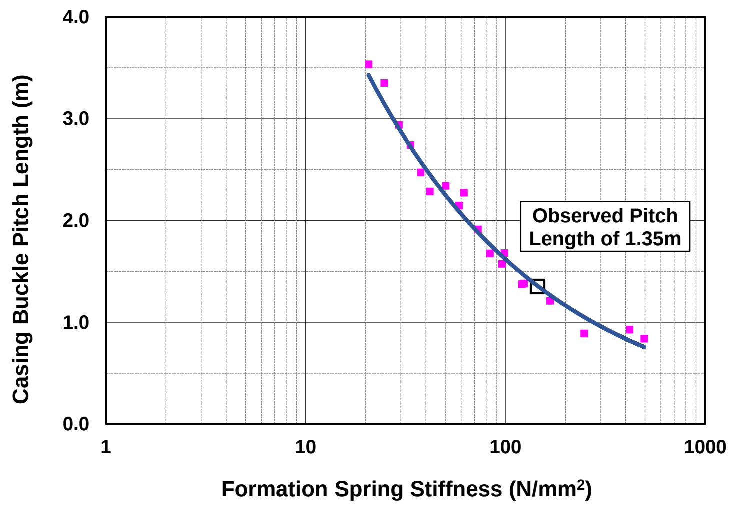


**Figure 8 Casing Buckle Pitch Length vs. Formation Stiffness**

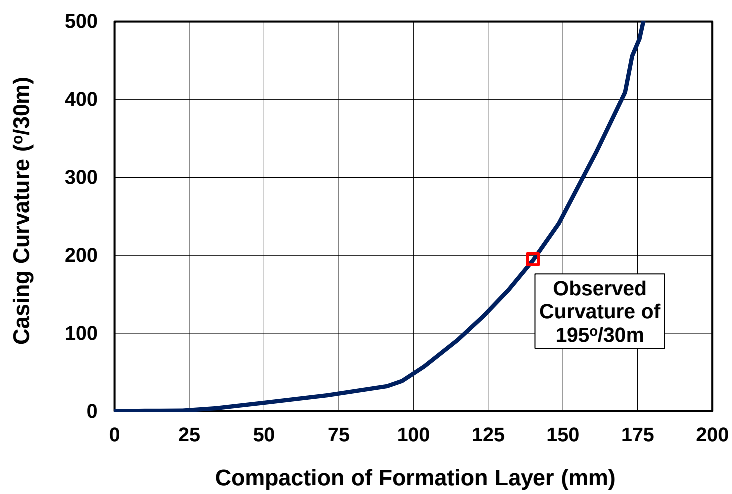

**Figure 9  Casing Curvature due to Buckling vs. Total Compaction Magnitude**

As shown in Figure 9, the casing curvature starts to increase significantly at a compaction displacement of 100 mm, which represents a uniform 1% compaction strain over the 10 m thick formation interval considered in the model.  The analysis results suggest that a formation compaction displacement of about 140 mm is required to match the observed casing curvature of 195°/30m.  Figure 10 shows the progression of the casing buckling deformation mode with the multi-wave buckle feature becoming more apparent above the 1% compaction strain level.

| | | | | | |
|---|---|---|---|---|---|
| 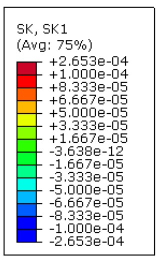  Curvature | 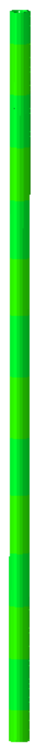 |  |  | 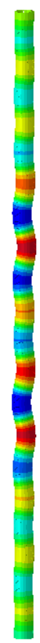 |  |
| Axial Strain | 0% | 0.71% | 1.15% | 1.40% | 1.73% |
| Curvature (°/30m) | 0 | 20.3 | 91.5 | 195 | 456 |

**Figure 10  Casing Curvature due to Buckling at Various Axial Compaction Strains**

Based on the casing curvature magnitude, the casing flexural strain can be calculated as the product of the curvature and the tubular radius.  In addition, based on the modeling assumptions, the casing axial strain matches the formation compaction strain. As described above, the sum of the flexural and axial strains equals the total strain. Assuming that the formation compaction occurs linearly as a function of time, the history response of the casing flexural, axial and total strains can be established as shown in Figure 11. The results suggest that the casing buckling initiated after 4 years of well operation. At 5.8 years, with the formation compaction displacement reaching 140 mm, the total casing strain is 2.41%, which exceeds the casing strain design limit of 1.5%, as proposed by Xie (2006). Therefore, based on this assessment, the structural and leakage integrity of the casing string (particularly the connections) may be considered at risk at 5.8 years.

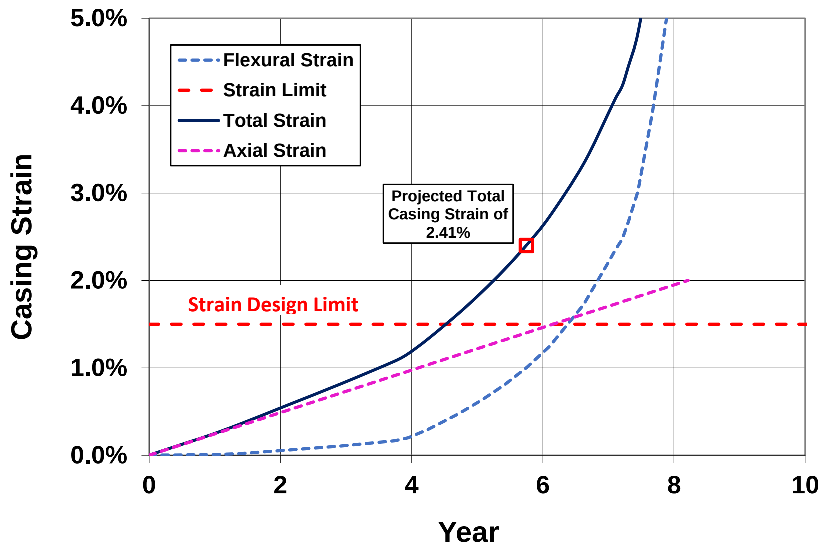


**Figure 11 Casing Strain due to Buckling**

## 6. Analysis of Casing Shear

### 6.1 FEA Model for Casing Shear

Field experience has demonstrated that formation shear movement represents a very severe casing load condition that is frequently encountered in the following types of field developments, wells and/or reservoir conditions (Dusseault et al. 2001): thermal cycle and SAGD operations which introduce high strain gradients through the reservoir cap rock and overburden section; multi-fractured horizontal wells in shales where the cumulative stimulation energy causes pre-existing fault activation or slippage on weak bedding planes; and reservoirs prone to significant subsidence or compaction in which case the shear movements tend to occur at both the reservoir top and in uphole formations in areas adjacent to the edges of the subsidence bowl created by production from several wells in a particular area. Entire well pads can be at risk in cases where the induced formation slip movement intersects the paths of many wells at depth. Therefore, it is very important to take potential formation shear movements into consideration with respect to casing design and wellbore construction in such applications. For example, according to published statistics, approximately 90% of the well casing failures in some thermal well fields in Western Canada can be attributed to shear movements induced in susceptible formations by the recovery process (Zahacy, 2015). Relative formation shear displacements with magnitudes of 25 mm or more have been reported in these fields and the majority of the failures occurred at connections.

Figure 12(a) presents a schematic diagram of the finite element model used to simulate casing-formation interaction under formation shear loading conditions. Typically, the shear plane is assumed to be located at the mid-height of the casing model reflecting the interface (or bedding plane) between two distinct formation layers. The layers may be comprised of similar materials or completely different materials (e.g. sand and shale layers). In the FEA model, the casing string is represented by either 2D or 3D beam elements (3D beam elements are required in modeling formation shear in situations where the formations properties vary in the radial direction), and the formation is represented by a series of soil springs. The shear displacements are applied to the soil-end nodes of the soil spring elements, with the movements applied in the opposite direction over the two adjacent layers, thus forming a shear plane.

The properties of the transverse soil springs for each soil layer are defined by a force-displacement relationship (i.e. indenter curve), established through FEA simulations of a rigid-body pipe being pushed laterally through a representative formation block. Figure 12(b) presents the formation load vs. displacement relationship established for a 177.8 mm casing in both a stiff shale layer and a weak sand layer (i.e. these characterizations are made on a relative stiffness basis that considers the shallow formation setting). As shown in Figure 12(b), the estimated formation stiffness of the shale layer is significantly higher than that of the sand layer.

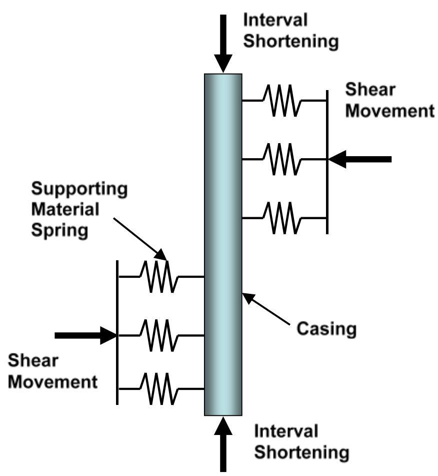


(a) FEA Model

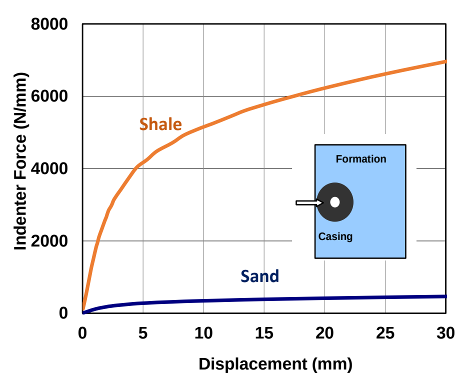


(b) Indenter Curve

**Figure 12 Schematic Diagram of FEA Model for Casing Shear Deformation and**

**Indenter Curve**

## 6.2 Example Case - Casing Shear

An illustrative example of casing shear deformation in a Western Canada thermal well application is considered here. Two different shear loading scenarios are examined to investigate the effects of different formation properties on the casing deformation response of a 177.8 mm, 34.2 kg/m L80 casing string: the first reflects shear plane development at the interface between two sand layers of equal stiffness, while the second considers shear movement between two shale layers of the same stiffness, but with a value that is much larger than that of the sand layers. Based on observations and analyses of numerous caliper logs run in such wells, shear deformations result in an in-plane offset or shift in the casing string axis with accompanying bending across the shear interval. This leads to the deformed casing having two adjacent but separate intervals with high bending curvatures in opposing directions. Both the separation distance between the two peak curvature positions and the peak curvature magnitude are highly dependent on the stiffness properties of the two formation layers adjacent to the shear plane as well as on the casing stiffness. Based on caliper log findings for casing shear deformations within representative lithological sequences, this shear analysis example will consider a peak curvature of 65°/30m in the sand layer scenario and 368°/30m in the shale layer scenario. The indenter curve relationships shown in Figure 12 were used for the sand and shale layers in the two respective analyses.

Figure 13 presents the peak casing curvature response established from the FEA results for the two scenarios as a function of the relative formation shear displacement. As shown in the figure, the casing curvature increases rapidly from the initial onset of the shear displacement in the shale scenario. In contrast, the casing curvature increases much more gradually. Given the same casing string was considered in both cases, this example serves to demonstrate that the significant difference in the response curves can be attributed solely to the stiffness and strength variation between the two formation materials. The substantial difference in peak curvature development also has significant implications in terms of internal diameter reduction (wellbore access limitation) and casing flexural strain levels – accordingly, these results indicate that shear displacements in shale (or relatively stiff material) intervals are much more serious from a well integrity and serviceability perspective. The relative formation shear displacements are 59.5 mm and 28.4 mm, respectively, for the 65°/30m and 368°/30m casing curvature conditions in the sand and shale cases.

Figure 14 presents the casing flexural strain response for the two soil type cases as a function of relative formation shear movement. The relative formation shear movements corresponding to the strain design limit of 1.5% are 138 mm for the sand interval and 25 mm for the shale interval. Note that the casing flexural strains are 0.34% corresponding to the 65°/30m casing curvature in the sand interval, and 1.91% corresponding to the 368°/30m casing curvature in the shale interval. This analysis confirms that for the cases defined by the representative caliper log surveys, the deformed casing string in the shale interval has experienced strain levels greater than the design limit, while the strain levels in the string deformed within the sand interval remain well below the design limit.

Figures 15 and 16 present contour plots of the casing curvature magnitude at a number of increasing shear displacement conditions for the sand and shale formation shear scenarios, respectively. For clarity, the deformations in these figures have been magnified by 10 times. As is evident from these two figures, the length of casing impacted by the shear displacement is much longer in the case of the softer and weaker sand material. The separation distance between the opposing peak curvature locations is 1.54 m for the sand layer case and 0.47 m for the shale case.

This example demonstrates that formation shear movement is a more critical loading condition for casing in formations with higher stiffness.

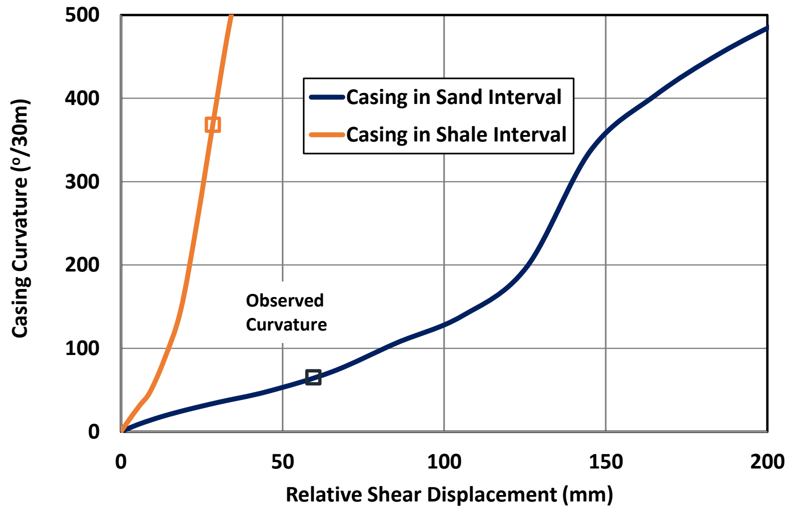


**Figure 13 FEA Results - Casing Curvature vs. Relative Shear Displacement**

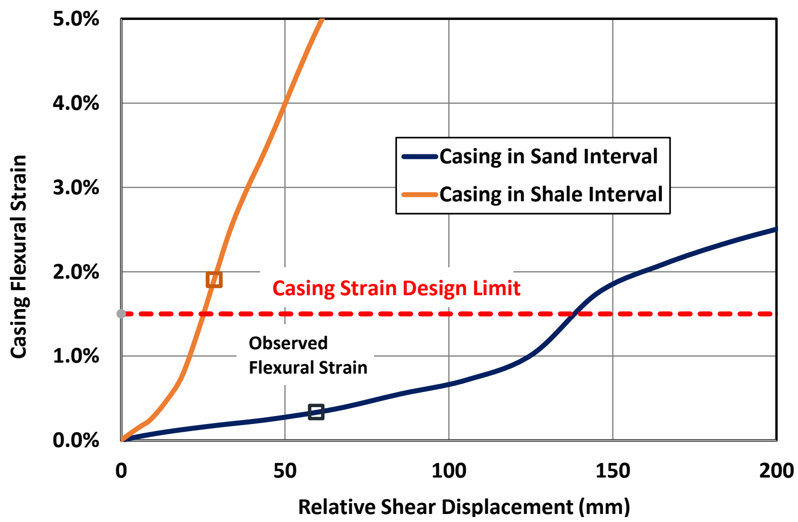

**Figure 14  FEA Results - Casing Flexural Strain**

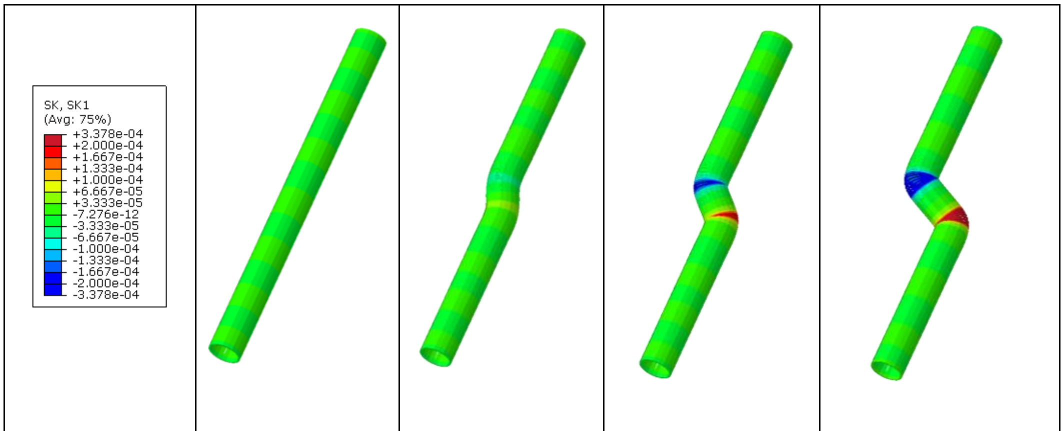


| | | | | |
|---|---|---|---|---|
| Shear Displ. (mm) | 0 | 65.4 | 145 | 266 |
| Curvature ($^o$/30m) | 0 | 72 | 338 | 581 |

**Figure 15  Casing Curvature due to Shear at Various Levels of Shear Movement in Sand Interval**

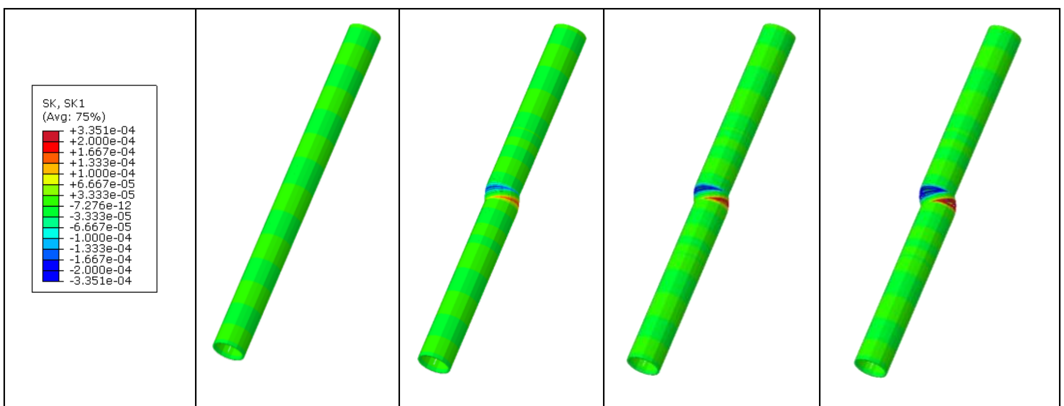


| | | | | |
|---|---|---|---|---|
| Shear Displ. (mm) | 0 | 23.4 | 28.4 | 38.4 |
| Curvature ($^o$/30m) | 0 | 249 | 368 | 576 |

**Figure 16  Casing Curvature due to Shear at Various Levels of Shear Movement in Shale Interval**

## 7. Conclusions

This paper presents several FEA models used to analyze three different types of well deformations, including casing collapse, buckling and shear. Corresponding analysis examples are used to demonstrate various approaches, each involving the application of FEA, that can be taken to investigate the nature and causal mechanisms of such deformations in conjunction with deformation feature characterizations established from casing caliper surveys run in actual wells.

The following conclusions are made based on the results from the FEA evaluations described in this paper:

- FEA can play an important role in the evaluation of casing deformations observed in oil and gas wells, leading to an enhanced understanding of the factors and conditions contributing to the occurrence and characteristics of such deformations, thus serving as a valuable tool for assessing failure risk and for identifying and screening practical mitigation strategies.

- High well temperatures and substantial axial tensile stresses can both have a notable impact on casing collapse resistance, and therefore these load conditions should be considered in the design of casing strings whenever they are relevant to the well application.

- Severe casing buckling can occur in weak formations under formation compaction loading conditions leading to high axial and flexural strains which can impact the structural and leakage integrity of the casing string. Therefore, casing buckling should be considered when designing wells for applications where subsidence or compaction may be anticipated to occur.

- Analyses of casing deformation response to formation shear loading conditions in soft and weak sand and relatively stiff shale layers demonstrated that the deformed casing shape and peak curvature magnitude was highly dependent on the stiffness properties of the formation material. The results indicate that shear displacements in stiff materials carry a much higher risk of causing wellbore access restrictions and high casing flexural strain levels, and, accordingly, such occurrences are much more serious from a well integrity and serviceability perspective.

## 8. Acknowledgement

The authors would like to sincerely thank their employer, C-FER Technologies, for supporting the work described in this paper and granting permission for its publication. The authors also acknowledge the work of several current and past colleagues in developing and enhancing the caliper log analysis software used to determine the casing deformation mode and amplitude for the field examples described in the paper.

## 9. References


1. Abaqus Users Manual, R.2016, Dassault Systémes Simulia Corp., Providence, RI. 2016.
2. API 5C3. Technical Report on Equations and Calculations for Casing, Tubing, and Line Pipe Used as Casing or Tubing; and Performance Properties Tables for Casing and Tubing. 2008.
3. Hetenyi, M., Beam on Elastic Foundations. University of Michigan Press. 1974.
4. DACC (Drilling and Completion Committee). In Situ Heavy Oil Operations – An Industry Recommended Practice (IRP) for the Canadian Oil and Gas Industry. Vol. 03. 2012. IRP 03:2012 (http://www.enform.ca/resources/detail/17/dacc-irp-volume-03-in-situ-heavy-oil-operations)
5. Dusseault, M.B., Bruno, M.S. and Barrera, J. Casing Shear: Causes, Cases, Cures. SPE Paper 72060. 2001.
6. Timoshenko, S. P. and Gere, J. M. Theory of Elastic Stability. Second Edition, McGraw-Hill Book Company. 1974.
7. Wagg, B., Xie, J., Solanki, S. and Arndt, S., "Evaluating Casing Deformation Mechanisms in Primary Heavy Oil Production", SPE 54116. 1999.
8. Xie, J., "Casing Design and Analysis for Heavy Oil Wells", World Heavy Oil Congress, Beijing, November 2006.
9. Xie, J. Casing Design for Compacting Reservoirs. World Oil Pore Pressure & Geomechanics, Houston, Texas, USA, September 13. 2007.
10. Xie, J. and Liu, Y. Analysis of Casing Deformation in Thermal Wells. 2008 ABAQUS Users' Conference, Newport Rhode Island, USA, May 19–22, pp. 542-553. 2008.
11. Xie, J. A Study of Strain-Based Design Criteria for Thermal Well Casings. 2008 World Heavy Oil Congress, Edmonton, Alberta, Canada, March 10-12, Paper 2008-388. 2008.
12. Zahacy, T. Examination of Thermal Well Reliability, Failures and Statistics, SPE Canada Heavy Oil Technical Conference, Calgary, Canada, June 9-11, 2015.